ELSEVIER

Surface Science 322 (1995) 293–300

surface science

The observation of oxygen disorder on the $V_2O_5(001)$ surface using scanning tunneling microscopy

Richard L. Smith, Weier Lu, Gregory S. Rohrer *

Department of Materials Science and Engineering Carnegie Mellon University, Pittsburgh, PA 15213, USA

Received 17 June 1994; accepted for publication 09 September 1994

Abstract

Constant current scanning tunneling microscope images of the $V_2O_5(001)$ surface were recorded in ultrahigh vacuum (UHV). The conductivity of the V_2O_5 crystal was increased by doping with Na during the crystal growth and flat surfaces were created by cleavage in N_2 or UHV. All images exhibit the 11.5 Å × 3.65 Å periodicity expected for a bulk terminated surface. However, images from different areas of the surface have different contrast and these variations are explained by assuming incomplete and inhomogeneous occupation of the vanadyl oxygen sites. This assumption is supported by image simulations which demonstrate that loss of the surface vanadyl O could account for the observed changes in contrast. Because these surface O vacancies are thought to influence the catalytic properties of the surface, their characterization is an important step towards understanding how the atomic-scale structure of a surface influences its properties.

Keywords: Scanning tunneling microscopy; Semi-empirical models and model calculations; Single crystal surfaces; Surface structure, morphology, roughness, and topography; Vanadium oxide

1. Introduction

There is a considerable body of experimental evidence supporting the idea that the oxidation reactions catalyzed by transition metal oxides are influenced by the atomic-scale structure of the surface and the defects that are present there [1–3]. Knowledge of the ideal and defective components of the surface structure is, therefore, a prerequisite for the development of models to explain the properties of these surfaces. The work described in this report was carried out with the objective of using scanning tunneling microscopy (STM) to determine the atomic-scale structure of the $V_2O_5(001)$ surface. This surface structure probe is preferred over low energy electron diffraction, which has been shown to alter the surface by initiating a topotactic structural transformation involving the evolution of oxygen [4].

Vanadium pentoxide has a layered structure composed of corner and edge sharing VO_5 square pyramids, as shown in Fig. 1. The oxygen atoms in this structure are coordinated by either 1, 2, or 3 V atoms and cleavage of the weak interlayer bonds produces the (001) surfaces that were examined in this study. This surface has several noteworthy geometric features that make it an interesting subject for an STM study. First, cleavage at the weak van der Waals bonds creates a binary surface with V atoms at the bases of the inverted pyramids and vanadyl O atoms at the apices of the upright pyramids. Second, the

* Corresponding author. Fax: +1 412 268 7596. E-mail: gr20@andrew.cmu.edu.

0039-6028/95/$09.50 © 1995 Elsevier Science B.V. All rights reserved
SSDI 0039-6028(94)00620-2

opposite orientation of the pyramids gives the surface a vertical corrugation of more than 2 Å from the vanadyl O position (the apex of the pyramid) to the exposed V atom position. Because this large vertical corrugation is caused entirely by the vanadyl O, vacancies should be easily detected in STM images as a substantial reduction in the surface corrugation. The surface vanadyl oxygens are especially significant because they are the first atoms removed during reduction reactions and they are thus thought to play a role in catalytic processes [5].

In its pure form, V_2O_5 is an insulator with an approximately 2.3 eV bandgap. However, it becomes conductive when an ion-insertion reaction is used to dope the compound with a group IA atom [6]. For the experiments described here, we used single crystals intercalated with small amounts of Na ($Na_{0.003}V_2O_5$). The Na atoms are situated in the interlayer spaces of the crystal and because their concentration is low, they do not have a significant effect on the bulk structure. However, because they act as shallow donors, they make the crystal semiconducting and suitable for high resolution STM measurements. The preparation and characterization of these samples is described in detail in Section 2.

Although atomic-scale resolution images of different transition metal oxide surfaces are being reported with increased frequency, the interpretation of the contrast in these images remains a challenge [7–14]. Nonstoichiometry, structural complexity, surface disorder, and uncertainties regarding the bonding and termination layers can all frustrate im-

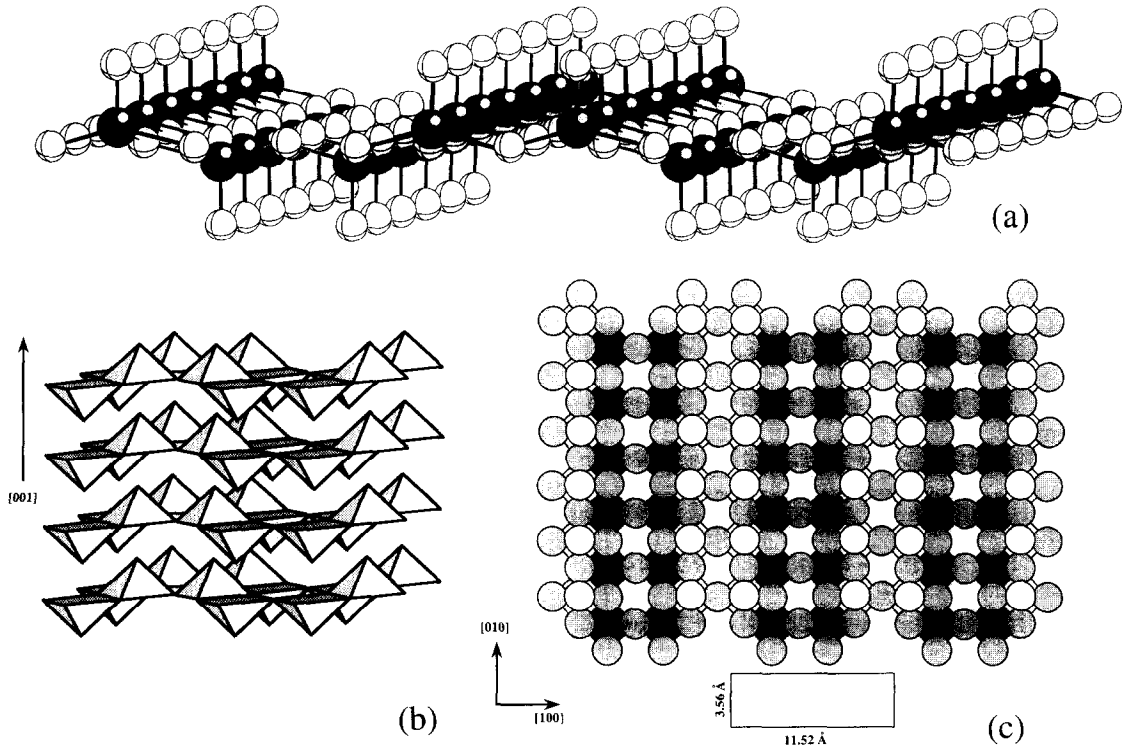

Fig. 1. The unit cell of V_2O_5, described in space group Pmmn (No. 59), contains two formula units and has the dimensions $a = 11.52$ Å, $b = 3.56$ Å, and $c = 4.37$ Å. (a) An oblique projection of a single layer of the V_2O_5 structure with an exposed (001) surface. The dark spheres are V and the lighter ones are O. The singly coordinated O atoms projecting upward from the surface are the so-called vanadyl O. The V are in a distorted square pyramidal coordination. (b) A polyhedral model of the extended structure, assuming ideal pyramids. Because there are no primary bonds connecting adjacent layers, crystals cleave easily perpendicular to c. (c) A projection on (001). Larger spheres are O and smaller (black) spheres are V. The O are shaded according to relative height, lighter indicating higher. The repeat unit is shown below.

age interpretation. In this paper, we test a variety of surface structure models against the STM observations by simulating the contrast that would arise from different proposed surface structures.

2. Experimental procedure

2.1. Sample preparation and characterization

Single crystals of $Na_{0.003}V_2O_5$ were prepared by the chemical vapor transport of powdered $Na_xV_2O_5$. $Na_xV_2O_5$ was prepared by combining 0.5 g of V_2O_5 (99.2% Johnson Mathey) with a 0.1M aqueous solution of $Na_2S_2O_4$ and stirring the mixture for 0.5 h at room temperature. After the powder settled, it was separated from the solution and washed with distilled water and acetone. The powder was then transferred to a quartz tube and flamed in vacuum to drive off residual water and solvent. The tube containing the dried powder was then vented in a N_2 filled glove bag, a small amount (approximately 0.05 g) of $TeCl_4$ was added, and finally the tube was re-evacuated and sealed to form an ampoule with an 8 mm diameter and a 55 mm length. The tube was then heated in a horizontal tube furnace where the temperature was graded from 530°C at the hot end of the tube to 500°C at the cool end. After 7 days, several large crystals that had been transported to the cooler end of the tube were harvested and stored in N_2.

Selected crystals were pulverized for X-ray diffraction analysis. The powder pattern showed that the structure was essentially identical to that of pure V_2O_5 and no impurity phases were detected. The lattice constants of the orthorhombic cell, determined by a least squares refinement of the 15 peak positions, were $a = 11.4959(95)$ Å, $b = 3.5510(51)$ Å, and $c = 4.3569(25)$ Å. The measurements indicate that the volume of the $Na_{0.003}V_2O_5$ cell is 0.5% smaller than the volume of the pure V_2O_5 cell. It is likely that the Na increases the strength of the interlayer bonding and causes this small contraction. Analysis of the sodium content by flame emission spectroscopy indicated that the chemical composition of these crystals was $Na_{0.003}V_2O_5$. The electronic conductivity, determined using a four-point probe method, was 0.04 $\Omega^{-1} \cdot cm^{-1}$. Taken together, the structural, chemical, and electrical measurements are all consistent with the model that the single crystals, grown by chemical vapor transport, are essentially V_2O_5 with a small amount of sodium intercalated into the interlayer spaces. The intercalated Na increases the electronic conductivity by creating a shallow population of donors, but does not significantly alter the structure.

2.2. STM measurements

All the STM measurements described in this paper were carried out in an ultrahigh vacuum chamber with a base pressure below 10^{-9} Torr. Before analysis, the crystals were cleaved either in the chamber, or in a N_2 filled glove bag connected to the chamber by a load lock. Several (001) surfaces of different crystals were imaged in the constant current mode using clipped Pt–Ir tips. High resolution images could be obtained using tunneling currents between 0.6 and 1.0 nA and sample biases between 2.0 and 3.0 V (tunneling to unoccupied sample states). The images presented here are representative of many observations, 50 of which were recorded. It was not possible to correlate the observed inhomogeneities (described in Section 3) with the crystal or the method of cleavage. High frequency noise (smaller than 2 Å) and a background plane have been subtracted from each image.

2.3. Contrast simulation

The contrast in constant current STM images was simulated using a method described in an earlier report [13]. Basically, the tunneling current was calculated as a function of the tip's lateral and vertical position over the sample by assuming that each atom in the model contributes independently to the tunneling current and that at any specific coordinate, the tunneling current (I) is given by a superposition of these contributions as follows.

$$I = \sum_i D_i \exp\left(-1.025 S_i \sqrt{\phi}\right)$$

S_i is defined as the distance between the surface of the tip (a sphere with radius r_{tip}) and the surface of the ith atom which is a hard sphere whose size is defined by the ionic radius. Although not explicitly in the equation for the tunneling current, the tip

radius influences the current through its effect on the separations, S_i. D_i is the relative contribution of the ith atom to the total density of electronic states in the conduction band (the band being probed in the STM images). For the tunnel barrier height, ϕ, we used a characteristic value of 1.6 eV. After determining the current at each position, constant current images can be easily extracted. Based on our experience using this model, the parameters that were found to have the most significant effect on the images are D_i and r_{tip}; the constant current level and the barrier height influence only the total vertical corrugation and do not substantially alter the appearance of the image or the shapes of features, since images are normalized to maximize contrast.

The term D_i is meant to represent, in the simplest possible way, the lateral variation of the surface density of states. For example, for a surface terminated by a single element, all D_i would be equal. For a binary surface layer, on the other hand, we would expect the density of conduction band states to be higher at the electropositive element and would weight the values of D_i appropriately. For the results presented in Section 3, we used a ratio of $D_V/D_O = 4$. In this case, we assume that in the upper part of the conduction band the V 3d states make a greater contribution to the conduction band than the O 2p states. We note, however, that variation of this parameter within reasonable limits (between 1 and 10) did not appreciably affect the image contrast. This computationally simple model allows a variety of parameters and structural models to be rapidly explored. While we do not expect quantitative accuracy, these simulations provide tangible manifestations of the often used qualitative arguments based on the convolution of geometric and electronic effects and they are thus useful to support interpretations.

3. Results and discussion

Constant current STM images of $Na_{0.003}$-$V_2O_5(001)$ are presented in Fig. 2. Assuming that the structure is bulk terminated, the surface repeat unit should be 11.5 Å × 3.6 Å (see Fig. 1c). Dimensions of the observed surface repeat unit, determined from Fourier transforms of the topographs, are consistent with the expected dimensions. Small differences in the repeat units are consistent with day-to-day differences in the thermal drift. This effect is amplified in the images in Fig. 2 because the primary corrugation is nearly perpendicular to the slow scan direction. Despite the fact that all of the images have essentially the same surface repeat unit, there are characteristic differences.

The predominant features of the image in Fig. 2a are the lines of light and dark contrast that run parallel to the b-axis. The lines of lighter contrast are approximately 5 Å wide, they have an 11 Å period, and a 2 Å corrugation. A smaller corrugation, within these lines of lighter contrast, has a periodicity of 3.6 Å and an amplitude of only 0.3 Å. Similar lines of lighter contrast, parallel to the b-axis, are found in image in Fig. 2b, but they are approximately half the width of those in Fig. 2a. Finally, these lines appear to be absent from the image in Fig. 2c and the corrugation parallel to the b-axis is now the largest. It is important to recognize that the vertical resolution from black-to-white in Fig. 2a is 2.25 Å, in Fig. 2b is 1.5 Å, and in Fig. 2c is 1.0 Å. The images in Figs. 2a, 2b, and 2c were selected as nearly homogeneous examples of three characteristic contrast types: images that have large corrugations as in (a), intermediate corrugations as in (b), and small corrugations as in (c). The image in Fig. 2d, displayed with 2.25 Å of vertical resolution, is representative of inhomogeneous areas that were also observed. Notice that the lines of white contrast parallel to the b-axis are similar to those in Fig. 2a, but they are not continuous. Thus, there is a low corrugation region in the central part of the image, bounded by high corrugation regions.

Because these images were recorded under the same conditions, the only plausible explanations for the different observations are changes in the tip structure or inhomogeneities in the surface structure. An explanation based on changes in the tip structure seems dubious considering images such as the one in Fig. 2d, which shows two different contrast types imaged by the same tip. Furthermore, the observations were reproduced with more than one tip. It is more likely that the differences in the images actually reflect disorder on the surface. In fact, the observations can be accounted for by assuming disorder in the vanadyl O positions. Based simply on a

model for the ideal atomic structure of the (001) plane, as illustrated in Fig. 1, we expect corrugations on the order of 2.0 Å over the vanadyl O positions, as seen in Fig. 2a. Furthermore, because the atoms occur in pairs, separated by about 4 Å, we expect the contrast from these species to be at least this wide (see the projection in Fig. 1c). Thus, the features in Fig. 2a are easily explained if we assume that the vanadyl O are the source of the white contrast. The image in Fig. 2c, on the other hand, would represent the case when both vanadyl oxygens are missing from the surface and the image in Fig. 2b represents an intermediate case where approximately one O in each pair of the vanadyl O is missing.

The arguments described above are based simply on the expected geometry of the surface and the measured corrugations in the topographic images; it was assumed that contrast effects due to the surface

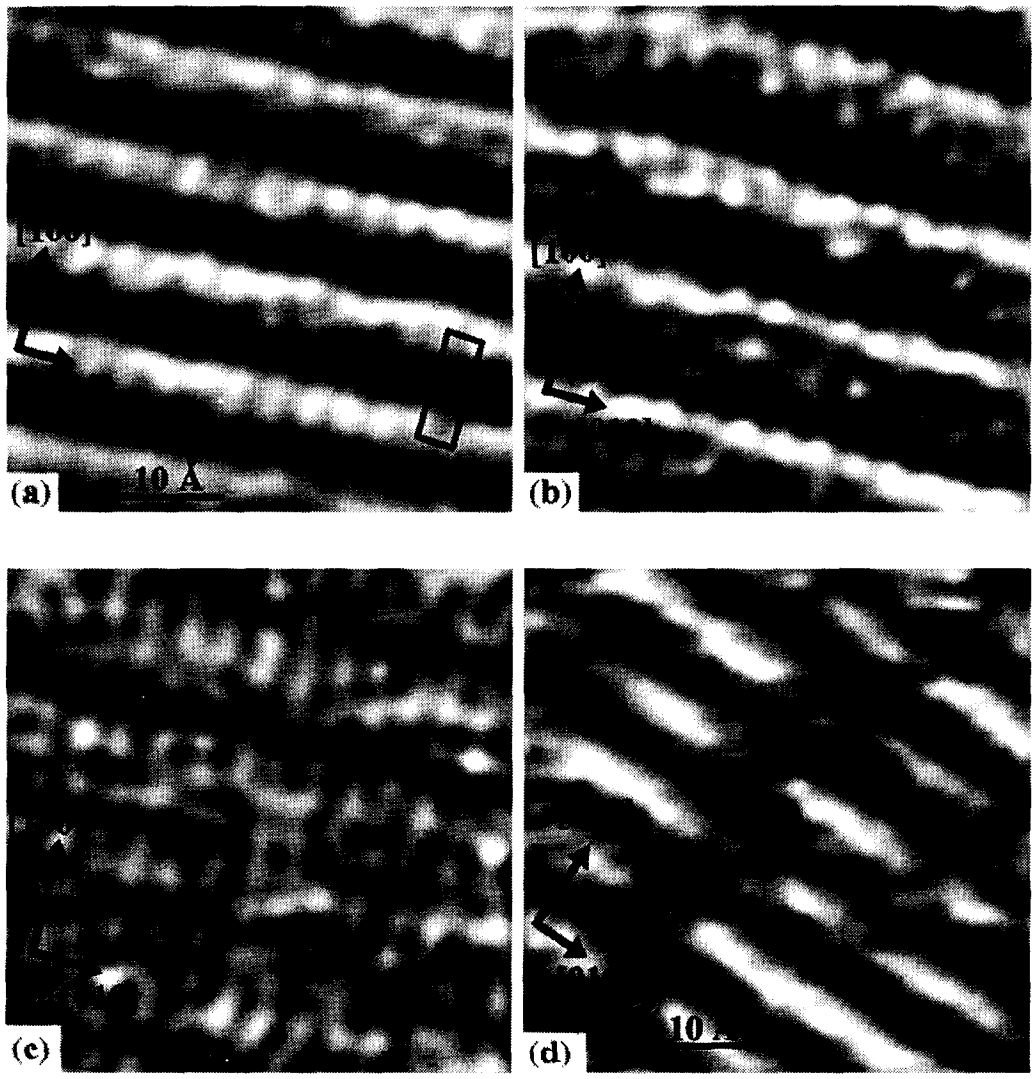

Fig. 2. Four constant current STM images of the V_2O_5(001) surface. Images (a), (b), and (c) have the same scale and orientation. The image in (d) covers a slightly larger area and has a different orientation. The surface repeat unit is indicated by the rectangle in (a). The vertical scale from black-to-white is in: (a) 2.25 Å, (b) 1.5 Å, (c) 1 Å, and (d) 2.25 Å.

electronic structure play a subordinate role. Because this conclusion is contrary to the conventional wisdom, it deserves further elaboration. It is often assumed that when tunneling into the empty states of a transition metal oxide, the tip is sensitive only to the metal atoms. The reasoning is that the conduction

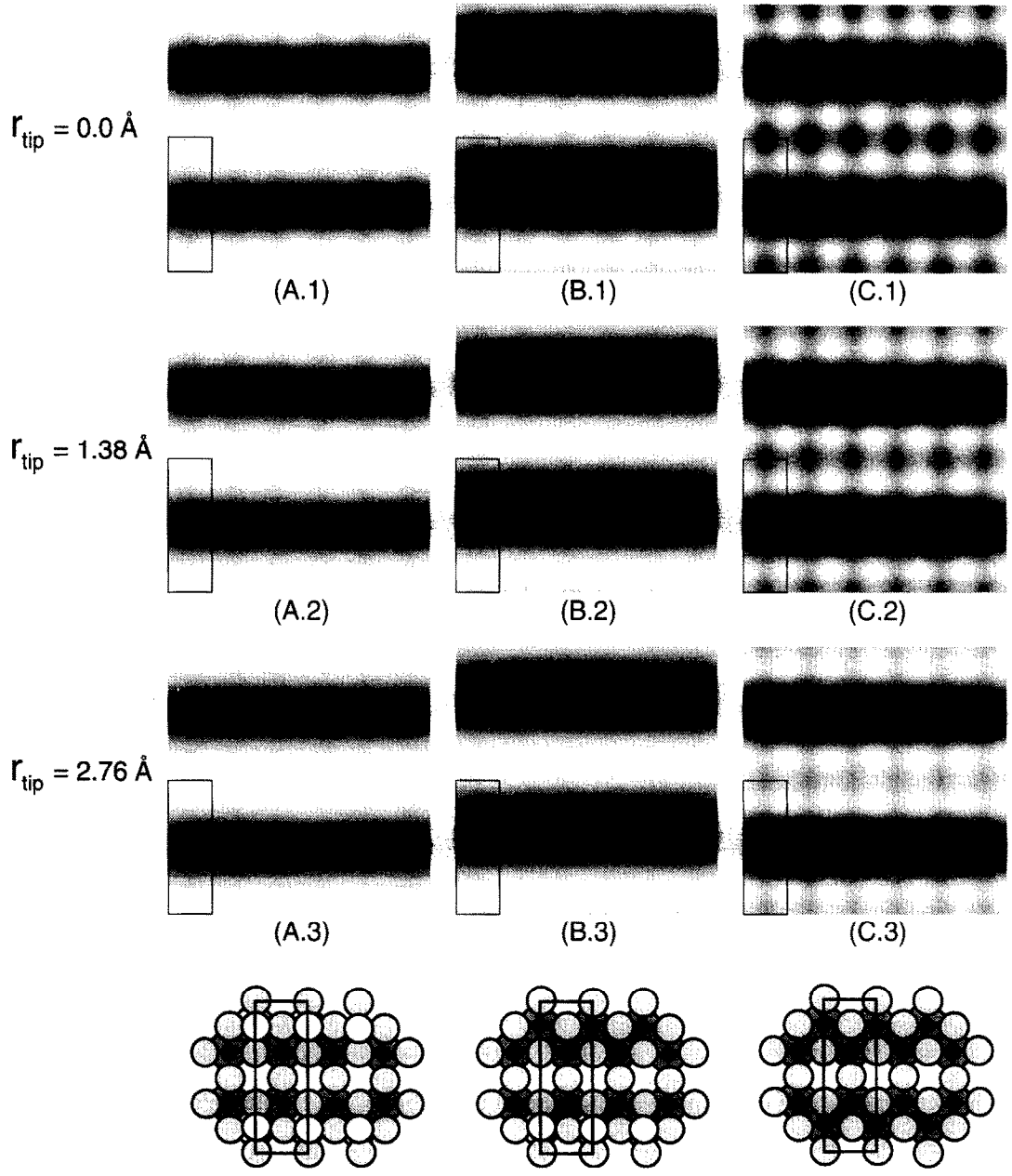

Fig. 3. Simulated constant current images, 23 Å × 21 Å. The images labeled A.1–A.3 are for the ideal surface, with all of the O in place. Each image is computed using a different tip radius (specified on the left) and assuming that $D_V/D_O = 4$. The images labeled B.1–B.3 were computed under the same condition, but it was assumed that half of the vanadyl O are removed. The images in C.1–C.3 were computed using a model in which all of the surface vanadyl O were removed. Projections of each of the models, using the same conventions as in Fig. 1c, are shown below the simulated images.

band is formed primarily from the cation d-orbitals. In this case, however, two important facts must be taken into consideration. First, the vanadyl O position is 2.5 Å closer to the tip than the exposed V atom. Second, while it is true that the cation orbitals dominate the density of states near the bottom of transition metal oxide conduction bands, the O 2p states make a significant contribution near the top of the band. Thus, the sensitivity to the O atoms increases when you tunnel near the top of the conduction band. Because the bonding in V_2O_5 is very anisotropic, its conduction band is relatively narrow (3.4 eV) [15]. Thus, these images were recorded by tunneling into states near the top of the conduction band where the sensitivity to O is increased.

To add support to our interpretation, we carried out contrast simulations which account for both electronic and topographic effects (see Fig. 3). Images were simulated assuming three different tips and three different surface structure models. The zero radius tip is meant to represent the high resolution limit. The other two radii, one times and twice the radius of a Pt atom, are thought to be more realistic. All other factors being equal, the model amplifies the V atom's contribution to the tunnel current by a factor of 4 ($D_V/D_O = 4$). However, because there is an inverse exponential dependence of current on separation, the larger size and adventitious positioning of the O ions on the ideal surface overwhelms the effect of the D_V/D_O ratio and, in this case, the O ions dominate the contrast.

Simulated contrast for the structural model with all of the atoms in their ideal positions (A.1 through A.3) shows an approximately 6 Å wide band of white contrast parallel to the *b*-axis. This band of contrast narrows when half of the O atoms are removed (B.1 through B.3). When all of the vanadyl O are removed (C.1 through C.3), the V atoms exposed by O removal create contrast similar to what is seen in the A series. However, because the V atoms are smaller and do not protrude from the surface as the vanadyl O do, the corrugations are much smaller. The corrugations in C are 1.3 Å smaller than those in A, similar to what is observed in the experimental images. Thus, the simulations support the interpretation that it is the vanadyl O that creates the contrast in the image in Fig. 2a and that exposed V atoms create the contrast in Fig. 2c. Changes in the occupation of the vanadyl oxygen position are responsible for the intermediate contrast in Figs. 2b and 2d.

The models reproduce the details of the contrast in the A and B series better than in the C series, where the surface O have been removed. This might be because the atomic coordinates used to calculate the simulations were taken from unrelaxed, bulk crystallographic data. This is probably a good approximation for the ideal surface (all O positions filled) that is formed by breaking the weak van der Waals bonds. This surface has a relatively low energy and, thus, the driving force for relaxation is small. However, when the vanadyl O atom is removed, it is unlikely that the V atom stays in the same position. Note in Fig. 1a that the V is elevated above the surface, effectively shortening the bond to the vanadyl O. Based on the results of pseudopotential calculations, Kempf and co-workers proposed that this bond has a significant degree of covalency [16]. After the vanadyl O is removed, it is reasonable to expect that the V would contract toward the surface into square planar coordination or possibly even below the surface, returning to a square pyramidal coordination (but with the pyramid inverted). In either case, we conclude that the loss of the vanadyl O leads to a flatter surface. Differences between the real (relaxed) structure and the ideal structure assumed in our model might account for the differences between the simulated and the experimental images.

Other recent STM observations of O disorder on transition metal oxide surfaces have involved crystals heated in vacuum, conditions where oxygen vacancy formation is expected [7,9,10]. Crystals for the experiments described here, on the other hand, were prepared by room temperature cleavage, so the disorder must be a result of the cleavage process or the STM measurement itself. Based on the data available at this time, it is difficult to specify the source of this disorder. Sequential images of the same area show no changes, apparently indicating that the scanning tip is not creating the vacancies. However, it is impossible to say what happens during the lower resolution scans that invariably precede the atomic-scale observations. Also, while cleavage induced termination layer variations have been observed for compounds with three-dimensional bond-

ing [12], anisotropically bonded compounds are expected to cleave uniformly at the van der Waals gap. This type of disorder has not been observed in STM images of other cleaved layered oxides [11]. Whatever the source of this disorder, it appears that the vanadyl O is very easily removed from the surface and that the vacancies are left behind in a nonuniform distribution.

Considering the physical and chemical properties of vanadium pentoxide, the observation of an oxygen deficient surface is not too surprising. For example, the energy for the formation of an oxygen vacancy, according to the reaction (written in the standard Kröger–Vink notation):

$$O_O = V_O^{\cdot\cdot} + 2e' + \tfrac{1}{2}O_2(g)$$

is known to be 1.3 eV, which makes it one of the most easily reduced transition metal oxides [17]. The fact that O is removed from the lattice with relative ease is, of course, related to the ability of V_2O_5 to catalyze the partial oxidation of hydrocarbons. In fact, it has been previously suggested that these vacancies play a role in the process [5]. Thus, by further characterizing the defect structure of this surface using real-space STM measurements, it should be possible to determine how the structure and properties of this surface are related.

4. Conclusion

Constant current images of the $Na_{0.003}V_2O_5(001)$ surface indicate that the atomic-scale structure is not uniform. Based on image contrast simulations, the inhomogeneities are assigned to disorder in the vanadyl O position. The O vacancies, which are created at room temperature, do not have a random distribution. There are regions where all of the vanadyl O atoms are in place and others where they are all missing. Because the surface vanadyl O vacancies are important for the selective oxidation of hydrocarbons, we believe that the characterization of their population and distribution by STM might provide insight into the relationship between the structure of this surface and its properties.

Acknowledgements

This work was supported by the National Science Foundation under Grant DMR-9107305. R.L.S. thanks the NSF Research Experiences for Undergraduates program.

References

[1] J.E. Germain, in: Adsorption and Catalysis on Oxide Surfaces, Eds. M. Che and G.C. Bond (Elsevier, Ansterdam, 1985) p. 355.
[2] M.K. Smith and U.S. Ozkan, J. Catalysis 141 (1993) 124.
[3] J. Haber, in: Solid State Chemistry in Catalysis, Eds. R. Grasselli and J. Brazdil (American Chemical Society, Washington D.C., 1985) p. 1.
[4] M.N. Colpaert, P. Clauws, L. Fiermans and J. Vennik, Surf. Sci. 36 (1973) 513.
[5] L. Fiermans, P. Clauws, W. Lambrecht, L. Vandenbroucke and J. Vennik, Phys. Status Solidi (a) 59 (1980) 485.
[6] P. Hagenmuller, J. Galy, M. Pouchard and A. Casalot, Mater. Res. Bull. 1 (1966) 45.
[7] G.S. Rohrer, V.E. Henrich and D.A. Bonnell, Science 250 (1990) 1239.
[8] R. Wiesendanger, I.V. Shvets, D. Bürgler, G. Tarrach, H.J. Güntherodt, J.M.D. Coey and S. Gräser, Science 255 (1992) 583.
[9] T. Matsumoto, H. Tanaka, T. Kawai and S. Kawai, Surf. Sci. 278 (1992) L153.
[10] P.W. Murray, F.M. Leibsle, H.J. Fisher, C.F.J. Flipse, C.A. Muryn and G. Thornton, Phys. Rev. B 46 (1992) 12877.
[11] G.S. Rohrer, W. Lu, R.L. Smith and A. Hutchinson, Surf. Sci. 292 (1993) 261.
[12] W. Lu, M.L. Norton and G.S. Rohrer, Surf. Sci. 291 (1993) 395.
[13] G.S. Rohrer, W. Lu, M.L. Norton, M.A. Blake and C.L. Rohrer, J. Solid State Chem. 109 (1994) 359.
[14] N.G. Condon, P.W. Murray, F.M. Leibsle, G. Thornton, A.R. Lennie and D.J. Vaughan, Surf. Sci. 310 (1994) L609.
[15] D.W. Bullet, J. Phys. C: Solid State Phys. 13 (1980) L595.
[16] J.Y. Kempf, B. Silvi, A. Dietrich, C.R.A. Catlow and B. Maigret, Chem. Mater. 5 (1993) 641.
[17] P. Kofstad, Nonostoichiometry, Diffusion and Electrical Conductivity in Binary Metal Oxides (R.E. Krieger, Malabar, FL, 1983) p. 57.